ES Materials & Manufacturing

RESEARCH PAPER View Article Online

Excellent Gas Barrier Properties PET Film Modified by Silicone Resin/Sericite Nanocomposite Coatings

YiFan Chen, Lei Ding, Bo. Jiang*, Li Liu, Yunzhe Du and YuDong Huang*

In order to improve the gas barrier properties of PET films, the intercalated sericite was used as a barrier material in the functional silicone resin coatings. Firstly, the functional silicone resin with excellent thermal properties and high crosslinking degree was prepared. Secondly, lamellar sericite was intercalated and characterized by SEM and XRD. It was found that the lamellar spacing changed to 1.053 nm, and the compatibility in silicone resin was improved. Finally, the water vapor permeability (WVTR) and the oxygen permeability (OTR) of the modified PET film were tested. The results showed that WVTR and OTR of the modified PET film reached 12.40 g/(m^2 • 24 h) and 29.91 cm^3/(m^2 • 24 h • 0.1 MPa) respectively, which indicated that the silicone resin modified by intercalated sericite successfully prevents the direct penetration of gas molecules, thus forming a "loop" when gas enters, prolonging its permeation path and effectively realizing high gas barrier performance.

Keywords: Barrier performance; Silicone resin coatings; Lamellar sericite

Received 18 March 2019, **Accepted** 17 April 2019

DOI: 10.30919/esmm5f216

1. Introduction

At present, with the improvement of the quality of life and consumption level, there are high requirements for food quality. The requirements for packaging materials are also higher than before. Gas barrier performance[1, 2] is one of the essential properties of food packaging materials. It is necessary to prevent oxygen and water vapor from entering the packaging interior and to prevent perfume and organic vapor from seeping out, so as to prolong the life of food.[3] In order to meet the gas barrier performance of PET food packaging film, a large number of modifications of PET film's surface have been carried out in recent years.[4] The main methods to improve the properties of PET films are multi-layer composite modification, coating modification, blending modification, surface evaporation modification and nano-composite modification and so on,[5-8] among which coating modification is the most time-saving and inexpensive method, and it can improve the gas barrier.[9,10]

Coating is a solid continuous film obtained by one-time coating. Gas barrier coating is a method of applying a layer of polymer coating liquid on the film to form a gas barrier coating.[11-13] At present, the functional silicone resin coating obtained by photo-thermal double curing technology[14-16] has the advantages of rapid curing, simple process, energy saving and environmental protection, and does not contain volatile solvents in the curing system, which is in line with the increasing emphasis on the environmental protection concept nowadays. This method can obtain transparent protective functional silicone resin coatings with excellent thermal properties and high degree of cross-linking. It can lay a foundation for improving the gas barrier properties of thin films.[17]

In addition, adding lamellar nanomaterials is also a common method for improving gas barrier property. At present, the common lamellar materials are lamellar nano-carbon materials[18-20] and lamellar nano-silicate materials.[21, 22] The nano-sheet material has a large contact area with the coating matrix, so it can effectively block the gas diffusion, thus becoming an ideal nano-filler to improve the gas barrier performance.[23-25] Sericite is a layered silicate with lamellar structure, stable structure and non-expansibility. It has excellent physical and chemical properties, such as high toughness and high strength. In addition, it is a two-dimensional structure with large specific surface area and high aspect ratio. This structure can effectively increase the gas diffusion path, reduce the diffusion rate and improve the gas barrier of the system.[26,27] Compared with lamellar carbon nanomaterials, sericite has the advantages of wide source and low price.[28-30]

In this paper, the gas barrier properties of PET films were improved by the functional silicone resin. The intercalated modification makes the interlayer spacing of the nano-sericite larger, so that the silica resin was inserted into the layered silicate. Finally, the layered silicate was evenly distributed in the silicone resin to form a class of nano-composite materials. By combining coating modification with nano-sheet materials, a "loop" structure is formed, which could increase the route of gas permeation through the film and further improve the gas barrier performance of the PET film.

2. Experimental

2.1 Materials

MIIT Key Laboratory of Critical Materials Technology for New Energy Conversion and Storage, School of Chemistry and Chemical Engineering, Harbin Institute of Technology, Harbin 150001, China
***E-mail:** jiangbo5981@hit.edu.cn*

Sericite was obtained from Chuzhou Yonghe Sericite Co., Ltd（Anhui China）, γ-glycidyl-ether-oxypropyl-trimethoxysilane (KH560), γ-methacryloxypropyl trimethoxysilane (KH570), trimethylolpropane-triacrylate (TMPTA) were purchased from Qufu Chengguang Chemical Co., Ltd（Shandong China）. N-dimethylaminoethyl-methacrylate (DMAEMA) was procured from Shanghai Tengquan Biotechnology Co., Ltd. 2-ethylBase-4-methylimidazoxane was supplied by Sarn Flower Technology Co., Ltd. Benzophenone was purchased from Beijing Brillingway Technology Co., Ltd. Cetyltrimethylammonium bromide (CTAB) and NaCl were procured from Shanghai Chemical Reagent Co., Ltd. Dense HNO_3 and ethanol were obtained from Xilong Chemical Co., Ltd. Polyether amine D230, hexanediol diacrylate (HDDA), sodium hydroxide were all got from Aladdin reagent Co., Ltd. All the reagents were used as received.

2.2 Modified sericite

The intercalation process of sericite consists of thermal activation, structural modification and intercalation modification.

The specific steps of thermal activation are to take appropriate amount of sericite (S) in alumina crucible and place it in muffle furnace for heating (room temperature to 200 ℃, heating rate is 5 K/min, then from 200 ℃ to 800 ℃, heating rate is 10 K/min), and then holding at 800 ℃ for 2 hours to obtain heat-activated sericite (S_h). Structural modification is to acidified and sodium-modification sericite. In order to obtain the acidified sericite (S_a), the 5 mol/L HNO_3 and S1 in a round-bottom flask with a solid-liquid ratio of 3% were stirred at 90 ℃ for 5 hours, and then washed by distilled water and filtered for many times. Sodium-modification sericite (S_s) was made from 3 wt% of S_a in a saturated solution of NaCl was stirred at 95 ℃ for 3 hours. The main process is intercalation modification of sericite (S_i).

Appropriate amount of CTAB and S_s were selected according to the molar ratio of CTAB/the CEC value (the CEC value of Sericite is determined by ammonium chloride-absolute ethanol method, and the pH value is adjusted to 7.) of sericite = 15. Water was used as solvent (twice the mass of CTAB) and pH value was adjusted to 4. Then it was stirred at 80 ℃, and reaction time was 24 hours.

2.3 Fabrication of matrix coating

The matrix resin was prepared by mixing the hydrolysate of bifunctional group (KH560+KH570) as prepolymer, HDDA as active diluent, TMPTA as crosslinking agent, benzophenone as photoinitiator, DMAEMA as co-initiator, E51 as adhesion regulator and polyether amine D230 as thermal curing agent. Modified sericite and unmodified sericite were added to the resin in different proportions for ultrasonic dispersion for 30 minutes. Then appropriate mixed liquid droplets were dropped to the PET film with a thickness of 48 um and coated on the coating machine. Finally, the resin system containing two sericite were cured by ultraviolet light and then cured by heat at 80 ℃. A gas barrier coating was obtained. In here, the thickness of the coatings obtained above is 20 um.

Preparation of silicone resin, modification of sericite and coating are shown in the Fig. 1.

2.4 Characterizations of modified sericite and silane coating

Empyrean Intelligent X-ray Diffraction (XRD) was used to measure the structural layer spacing of sericite before and after modification. The test conditions were lamp power 2.2 kW, copper target, λ = 0.15406, test range 0.5 mm-70 mm, scanning speed 2 °/min, step size 0.02°. Quanta 200 (FEI Co., America) scanning electron microscopy (SEM) was used to test the samples. Sample section treatment: The cured resin was ground repeatedly, then its surface was cleaned with acetone, and finally dried at 80 C. The obtained sections were characterized by SEM for the section morphology. The cured silane system was tested by thermo gravimetric analyzer (TG) TA-Q500 （America）. The sample is accurately weighed at about 10 mg. Under argon atmosphere, the temperature rises from room temperature to 800 ℃ at the rate of 10K/min, and the gas flow rate is 50 mL/min. When studying the thermal decomposition kinetics of silane system, the thermodynamic properties of silane system were analyzed by changing the heating rate, including 5 K/min, 10 K/min, 15 K/min and 20 K/min.

2.5 Characterizations of modified PET film

Gas barrier test includes moisture permeability test and air permeability test. Moisture permeability test: cut the sample membrane into A4 size area, use W3/031 water vapor permeability tester for 24 hours, test according to GB 1037. Air permeability test: cut the sample membrane into A4 size area, use Classic 2016 differential pressure gas permeameter for 24 hours oxygen permeability test, according to GB 1038. The water resistance of the modified PET film was tested according to the national standard GB/T1733-93.

3. Results and Discussion

3.1 Characterization of silicone coatings

In order to analyze the thermal properties of silicone resin coatings, the thermal decomposition process of TG of silicone resin obtained by photo-thermal double curing was studied at different decomposition

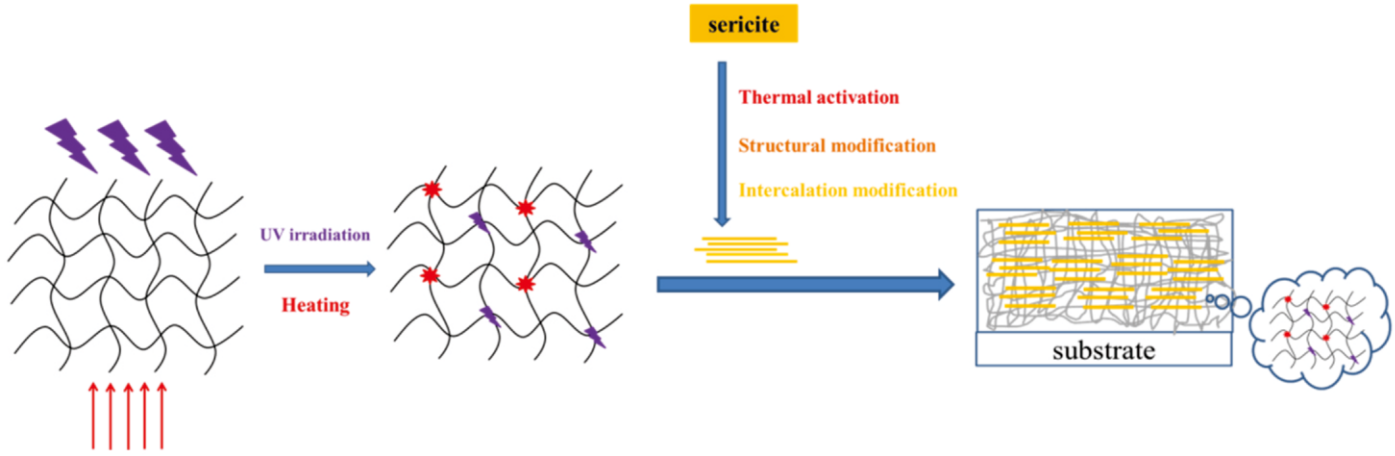

Fig. 1 The schematic diagram of the complete process.

rates. Here, the decomposition rate was changed by changing the heating rate. In this paper, the thermal decomposition of the coating system was studied at different heating rates of 10 ℃ /min, 20 ℃ /min, 30 ℃ /min and 40 ℃ /min. Fig. 2 is thermo gravimetric charts of the coating system at different decomposition rates.

From the DTG curve in Fig. 2, it can be seen that the maximum decomposition temperature of the silicone resin system is about 400 ℃. The first thermal weightlessness peak of silicone resin occurs at 270 ℃, which is caused by the dehydration of silicone hydroxyl group. Because the silicone resin system includes two parts of thermal curing and photo curing, there are two thermal weightlessness peaks at 360 ℃ and 450 ℃ respectively, which results in the rearrangement of silicone oxygen chains in the DTG curves at different temperatures.[31, 32] According to the above TG curves at different decomposition rates and combined with Ozawa method, logβ and 1000/T curves at different reaction degrees are obtained, as shown in Fig. 3.

Based on the scatter plots of logβ and 1000/T at different degrees of decomposition, the slope can be calculated by regression method. The activation energy required for the degradation reaction at different degrees of decomposition can be calculated at this time, as shown in Table 1 below.

It can be seen from the above table that when the degree of decomposition is small, the self-condensation of silicon hydroxyl group occurs, forming Si-O-Si bond and small molecule water, which requires low activation energy; when the degree of decomposition is large, that is, at the later stage of decomposition reaction, cage-like small molecules and ring oligomers are formed in the system, and the activation energy for chain breaking is high. Therefore, the coating system with excellent thermal performance has been obtained in this paper.

In addition, the functional silicone resin was treated by acetone extraction for 24 hours, and the mass percentage of the residue was used to characterize the crosslinking degree of the silicone resin system. From the table below, it can be seen that the residual percentage of photo-thermal double curing silicone resin after extraction reaches about 90 %, which indicates that the system has a high degree of crosslinking. In the photo-thermal double curing system, there are both double bond and epoxy crosslinking networks. Therefore, a double bond and epoxy network structure is formed in the double curing system. This crosslinking network structure greatly improves the crosslinking degree

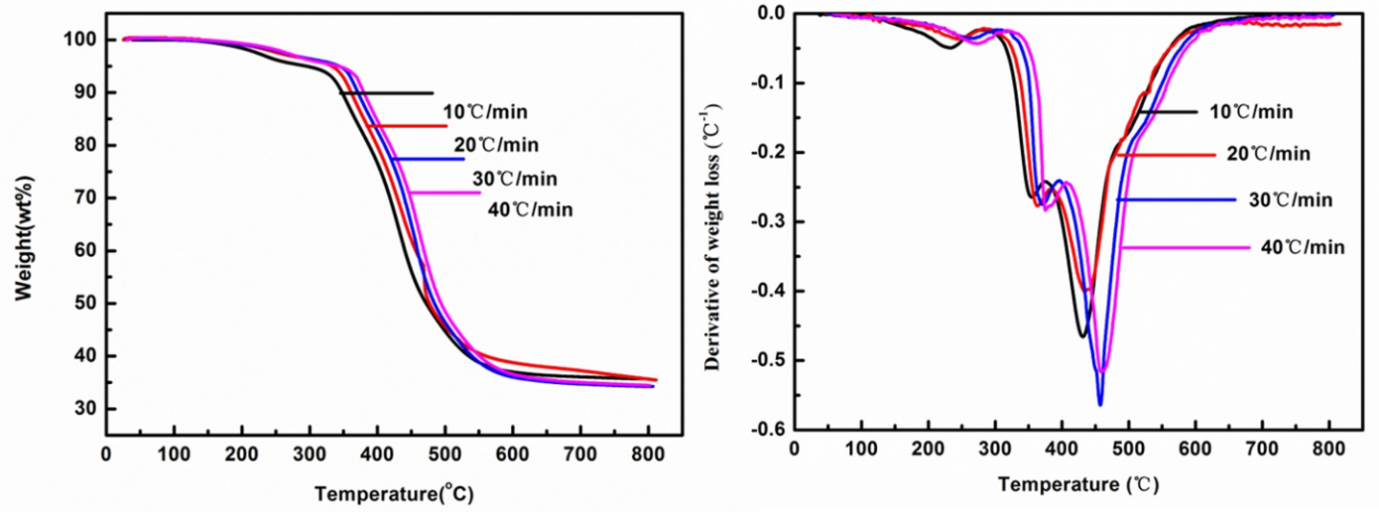

Fig. 2 TG and DTG curves of silicone resin system at different decomposition rates.

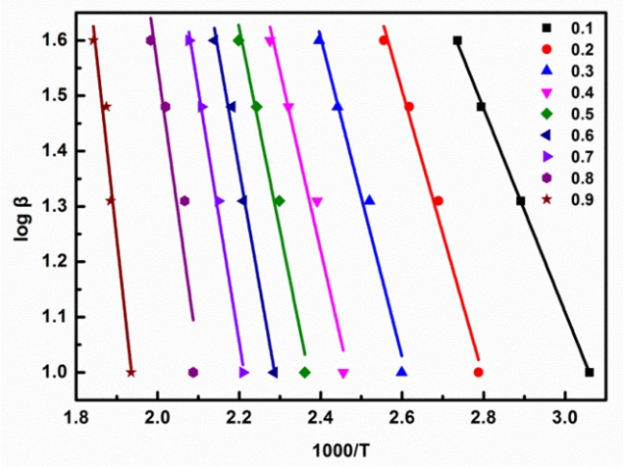

Fig. 3 Logβ and 1000/T curves at different reaction degrees.

of the system. The complex cross-linking structure and high degree of the cross-linking lay the foundation for improving the gas barrier of PET film.

In Fig. 4, comparing the gas barrier properties between the original PET film and the silicone coated PET film, the average water vapor permeability (WVTR) is 18.31 g / (m^2 • 24 h) and the average oxygen permeability (OTR) is 35.57 cm^3 / (m^2 • 24 h • 0.1 MPa), for the original PET film. However, the average water vapor transmittance was decreased by 1.32g / (m^2 • 24 h) and the average oxygen transmittance was decreased by 1.33 cm^3 / (m^2 • 24h • 0.1 MPa), for the coated PET films. It can be seen that the moisture permeability and air permeability of the coated PET films have decreased to a certain extent, which was attributed to the cross-linking structure of the coatings mentioned above and to lay the foundation for improving the gas barrier.

3.2 Characterization of modified sericite

From the XRD diffraction patterns (Fig. 5), it can be seen that the sharp degree of the diffraction peaks on the crystal faces (002) of S, S_h and S_i are obviously reduced, the peaks are gradually broadened and the intensity of the peaks is gradually reduced, which indicates that the crystallinity of sericite decreases and the integrity of crystal structure is destroyed from raw sericite to heat-treated sericite, then to intercalated sericite. From S to S_h, the peak intensity and the sharp degree of the diffraction peak decrease most obviously, which indicate that the crystal structure of sericite is distorted by high temperature heating, thus achieving a good effect of crystal activation. Generally speaking, the structure of sericite was modified and the lattice was activated after activation treatment, which laid a foundation for the intercalation modification of sericite.

In addition, the variation of lamellar spacing of sericite can be visually reflected by XRD spectra. For sericite, the interval between layers is reflected by the value of d002. According to Bragg equation,

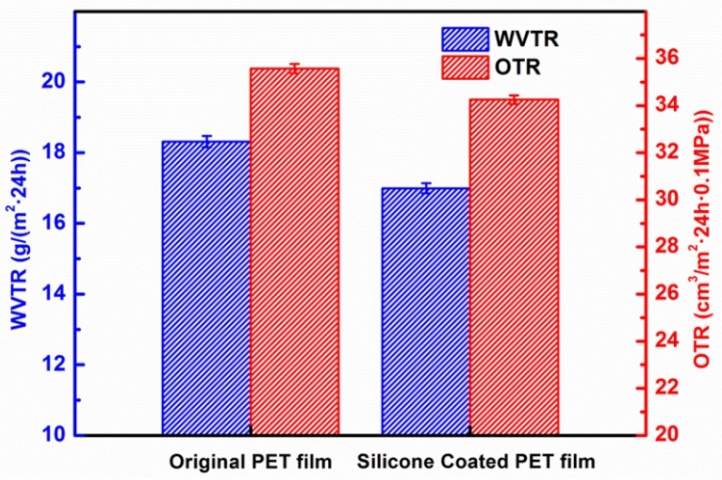

Fig. 4 WVTR and OTR of the original and the silicone coated PET film.

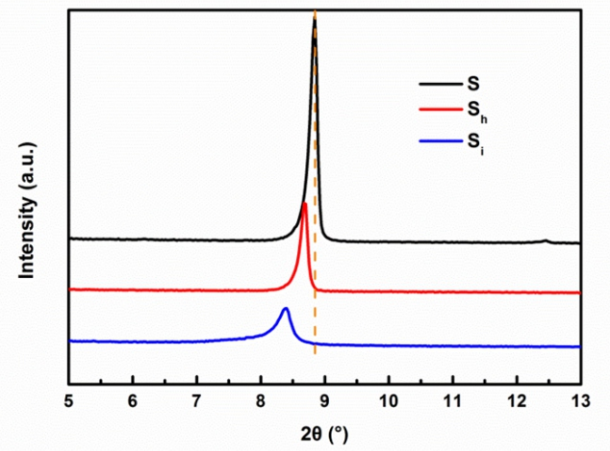

Fig. 5 Empyrean Intelligent X-ray Diffraction of sericite, heat-activated sericite and intercalated sericite.

Table 1 Activation energy of silicone resin system at different decomposition degrees.

Decomposition degree / α	Slope / k	activation energy / E（kJ/mol）
0.1	-1.840	33.503
0.2	-2.593	47.209
0.3	-2.885	52.525
0.4	-3.250	59.162
0.5	-3.663	66.687
0.6	-4.204	76.527
0.7	-4.540	82.638
0.8	-5.238	95.353
0.9	-6.688	121.757

Table 2 Initial mass, final mass and the mass percentage of the residue of silicone resin.

	Initial mass （g）	final mass （g）	the mass percentage
the photo -thermal cured silicone resin	1.007	0.909	90.27%

the interval between layers of lamellar structure can be calculated directly. The specific equation is as follows:

$$\lambda = 2\ d\ \sin\theta$$

Among them, d is the average distance between the silicate layers, θ is the half-diffraction angle, and λ is the wavelength.

From the above Table 3 and XRD spectra, it can be seen that with the activation process, the diffraction peak of sericite moves obviously to the direction of low diffraction angle (to the left), and the interlayer spacing increases continuously. This shows that the use of surfactant CTAB to intercalate sericite plays a role in enlarging the interlayer spacing, and lays a foundation for the uniform dispersion of sericite in the coating system.

Scanning electron microscopy analysis of sericite before and after intercalation modification shows that the structure of sericite before intercalation modification is compact. And the surface of sericite is smooth, the layers are clear, the diameter and thickness of sericite are large, and there is a tendency of aggregation in the natural state, as shown Fig. 6a. After intercalation modification, the crystal structure of the sericite lamellae remained intact, and a certain degree of dispersion and exfoliation were obtained, as shown Fig. 6b. The tendency of aggregation decreased in natural state.

The cured silicone resin was quenched, and the micro-morphology was analyzed. Scanning electron microscopy (SEM) images of acetone-cleaned sections show that sericite without intercalation treatment is not uniformly dispersed in the coating system, and there is obvious agglomeration, as shown Fig. 7a. Sericite with intercalation treatment is uniformly dispersed in the coating system and has good compatibility with the system, as shown Fig. 7b. By comparing the dispersion of sericite in the intercalated and un intercalated coatings, it can be seen that the intercalation treatment makes the sericite lamellae smaller, the lamellar structure looser, and the lamellar structure is more uniform in the system. This shows that the dispersion of sericite in the coating

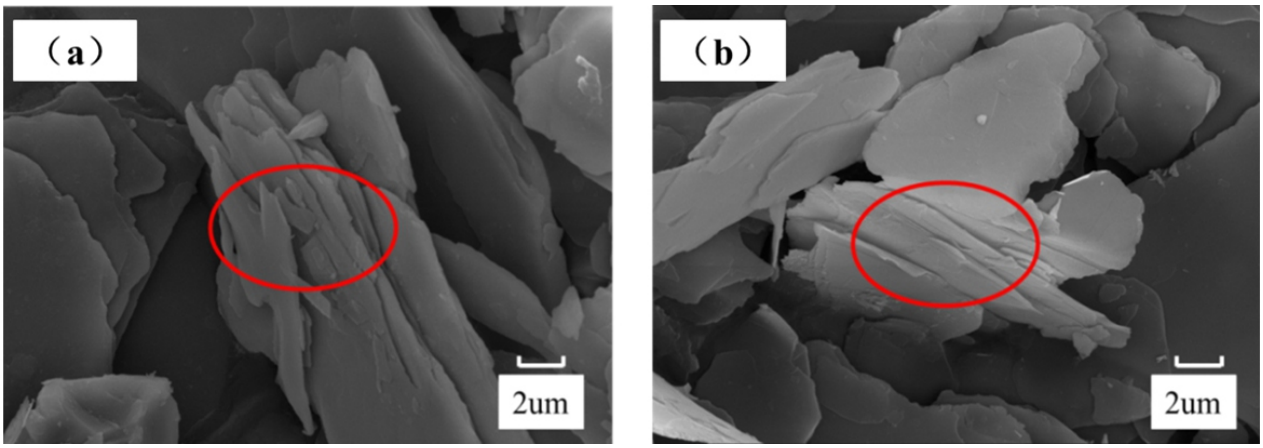

Fig. 6 Scanning Electron Microscope Section of sericite (a) and modified sericite (b).

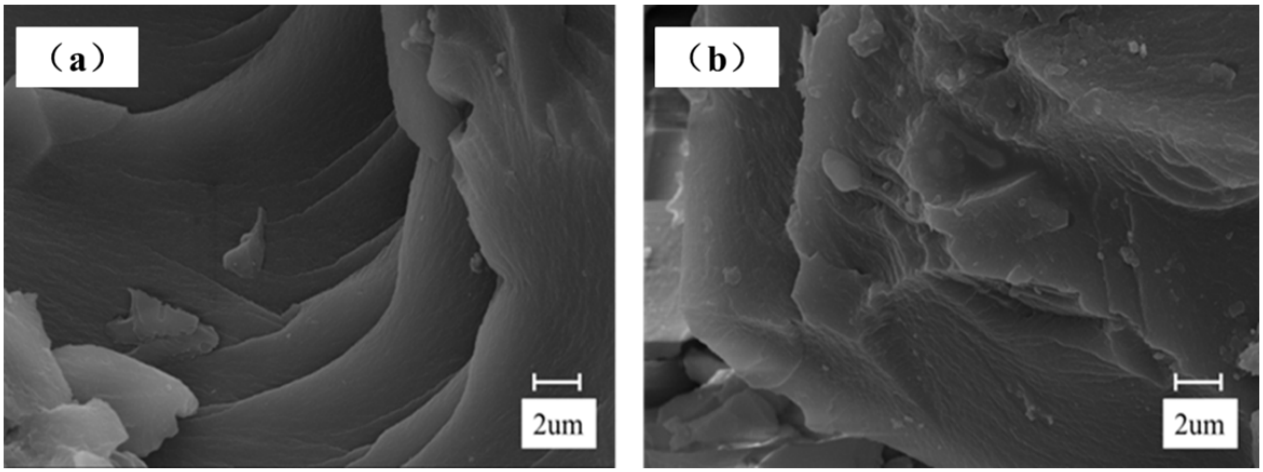

Fig. 7 Scanning Electron Microscope Section of sericite (a) and intercalated sericite (b) dispersion in resin.

Table 3 Interlayer spacing of sericite during intercalation modification.

	S	S_h	S_i
2θ	8.84	8.69	8.39
d/nm	1.000	1.016	1.053

system is improved by intercalation treatment.

3.3 Characterization of modified PET film

In order to study the effect of sericite as a barrier material on the gas barrier properties of coatings, the intercalated modified nano-particles sericite was added into the coatings at different proportions (0%, 0.5%, 1.0% and 1.5%) to modify the PET film coatings. And the gas barrier properties of the coatings were tested, including oxygen permeability test and moisture permeability test. The specific results are shown in Fig. 8.

For the original PET film, the average water vapor permeability is 18.31 g / (m^2 • 24 h), and the average oxygen permeability is 35.57 cm^3 / (m^2 • 24 h • 0.1 MPa). It can be seen that the water vapor and oxygen barrier property of modified PET film increases first and then decreases with the addition of sericite as the barrier material. When the content of sericite is to 1%, the gas barrier reaches the best state. The average permeability of water vapor is 12.40 g / (m^2 • 24 h), and the average permeability of oxygen is 29.91 cm^3 / (m^2 • 24 h • 0.1 MPa). The barrier of water vapor and oxygen increases because the filler sericite is dispersed in the coating system in a lamellar structure state. When the gas molecules encounter lamellar nanomaterials, they cann't penetrate, but change the direction of molecular diffusion, which makes the diffusion path in the coating become tortuous. This effectively prolongs the diffusion path of gas and slows down the diffusion rate, and thus reduces the gas transmission. The barrier property of the film is improved.[24] However, with the addition of barrier materials, the gas barrier has a decreasing trend. Considering that the optimum proportion of filler added to the coating is not more than 1%, the reason for the decrease of gas barrier may be due to the excessive amount of filler added, which leads to the decrease of the homogeneity of particles in the resin and cann't effectively prolong the gas diffusion path, and ultimately leads to the decrease of gas barrier.

In addition, in order to compare the effect of intercalation modification of sericite on gas barrier performance, the sericite without intercalation modification was added to the coating, and the gas barrier property was tested, and compared with the sericite with intercalation modification in the coating. The amount of the sericite added here is 1% of the optimum mass fraction of the above conditions. For convenience, the coated PET film added unmodified sericite was named as U-PET film, and the coated PET film added 1% modified sericite was named as 1%-M-PET film The results are shown in Fig. 9.

As can be seen from the above figure, the average water vapor

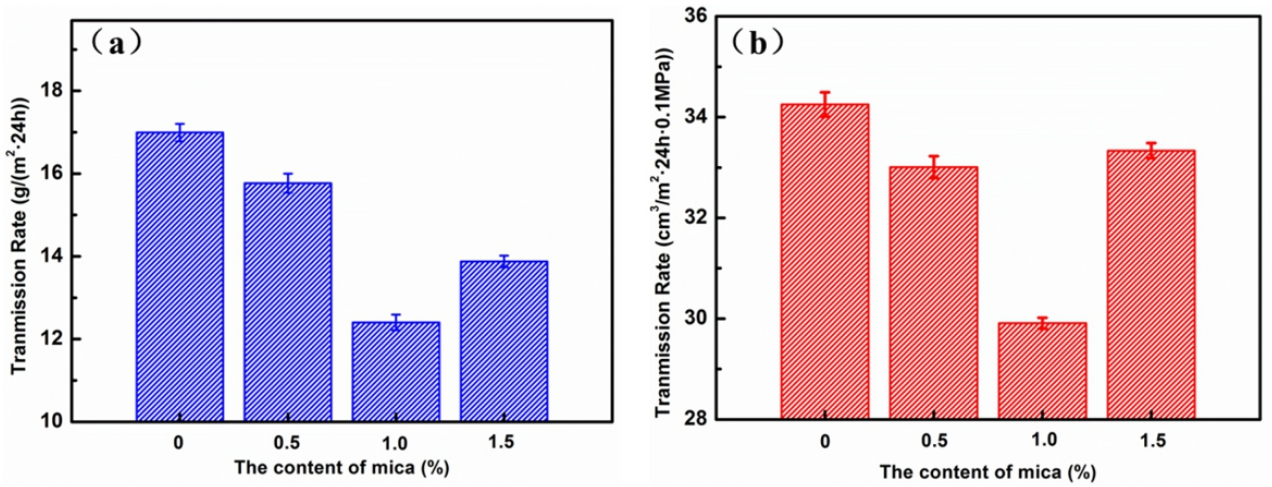

Fig. 8 moisture permeability (a) and oxygen permeability (b) of modification PET films.

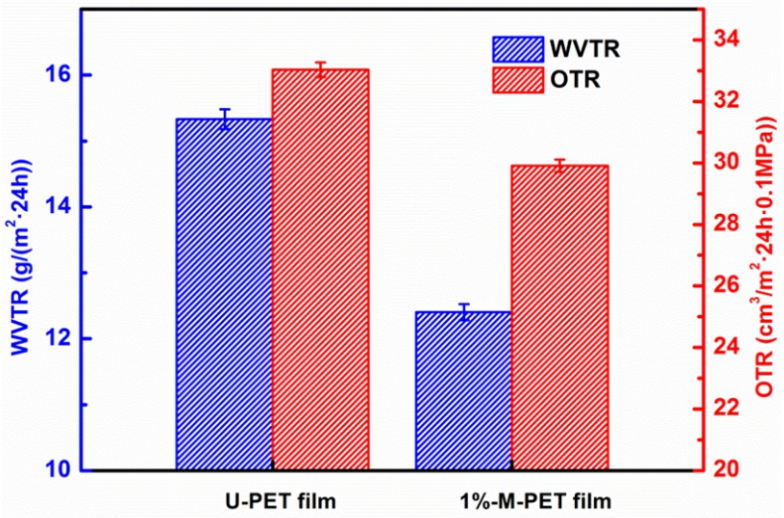

Fig. 9 moisture permeability and oxygen permeability of U-PET film and 1%-M-PET film.

permeability and oxygen permeability of silicone resin with unmodified mica are 15.33 g / (m^2 • 24 h) and 33.03 cm^3 / (m^2 • 24 h • 0.1 MPa). Comparing with the former, both water vapor permeability and oxygen permeability of silicone resin with modified mica decreased significantly. This is because the intercalation modification of sericite enlarges the interlayer spacing. When the gas passes through the coating, more layers of nanoparticles are encountered and the diffusion direction is changed many times. Thus the effective diffusion path of the gas is prolonged and the barrier property is improved.

By analyzing the diffusion model of gas in three coating systems, it can be found that adding intercalated lamellar sericite into the coating can effectively increase the path of gas passing through the coating, thus increasing the diffusion time and effectively improving the gas barrier performance of the coating.

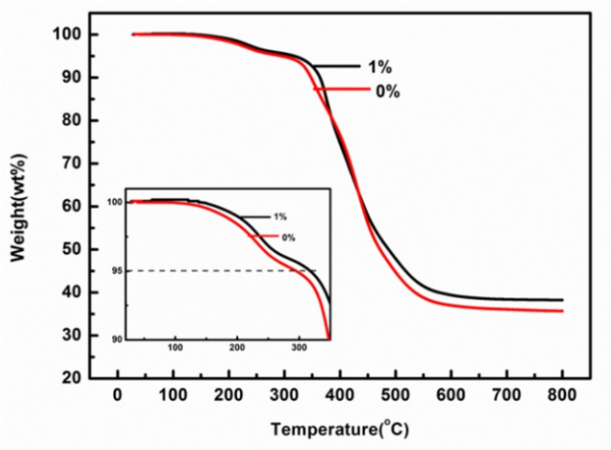

Fig. 10 Simple silicone resin coating and silicone resin coating of modified sericite with 1% addition.

In addition, the resin with the best mass fraction (1%) of sericite was added and its thermodynamic properties were analyzed. As can be seen from Fig. 10, the coating with sericite and without sericite has similar TG curve. In this paper, the initial decomposition temperature of coatings with sericite is 319 °C, and that the coatings without sericite is 295 °C. The initial decomposition temperature of the coatings increased by 24 °C after adding sericite, which indicated that the addition of sericite increased the thermodynamic properties of the coatings to a certain extent.

3.4 Gas barrier mechanism of sericite in coatings

From the results of the influence of sericite on the gas barrier properties, the gas barrier properties of the films were obviously improved by adding the barrier materials. Therefore, a theoretical model of gas diffusion was established based on the influence of sericite on the gas barrier properties, and the barrier mechanism of sericite in the coatings was further analyzed.

When there is no barrier layer material in the coating, the gas diffuses directly in the coating and passes through the coating, thus the gas diffusion path is the shortest. After adding barrier lamellar materials, gas molecules cann't penetrate the two-dimensional nano-lamellar structure, but change direction and diffuse in a zigzag way. The gas path changes from direct penetration to "loop" form, which extends the route of gas entering the coating and slows down the diffusion speed of gas molecules.[24] This effectively improves the barrier performance of the coating. Specifically as shown in Fig. 11.

When there is no barrier material in the coating, the path of gas penetration through the coating is directly the thickness of the coating,

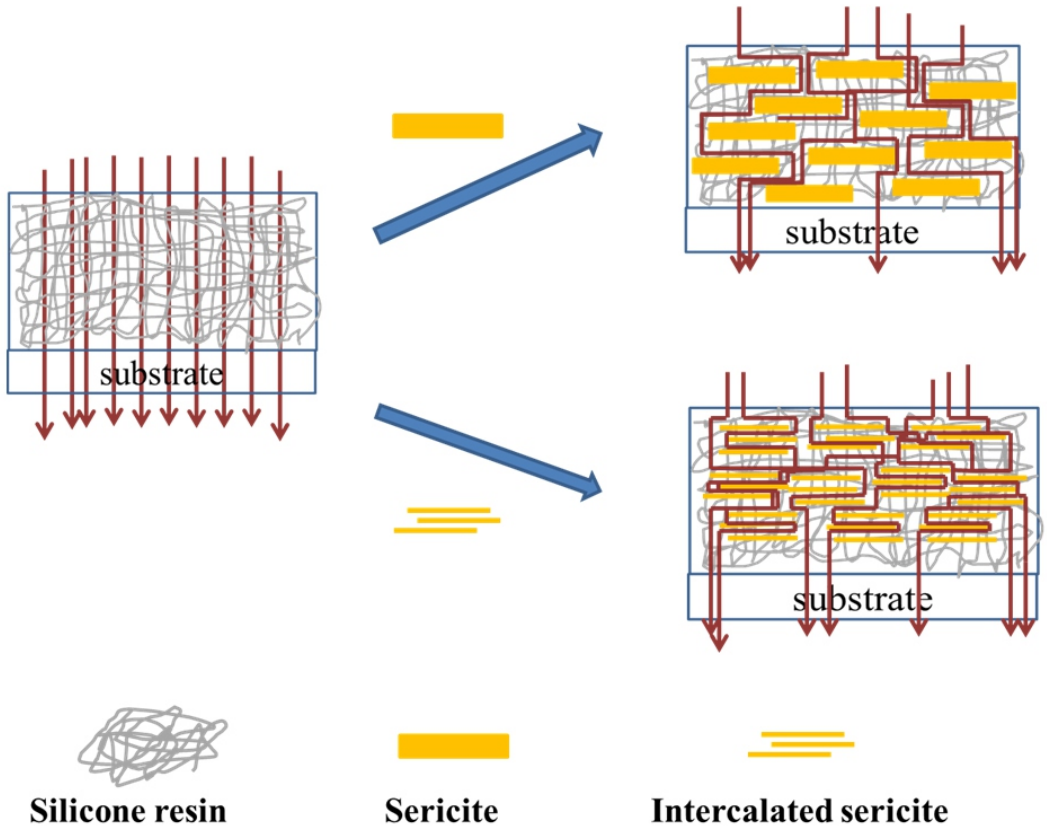

Fig. 11 Path diagrams of water vapor or oxygen penetrating thin films.

and the gas penetrates the coating directly from the figure above. The direction of gas diffusion through the coating is changed due to the obstruction of the lamellar structure when untreated sericite is as a barrier material in the coating. The path of penetration becomes tortuous and increases the transverse path, so the path of gas penetration through the coating is that the thickness of the coating adds the transverse diffusion length.[33] The path of gas penetration through the coating is still the thickness of the coating add the transverse diffusion length with the intercalated lamellar sericite.[34, 35] However, the enlargement of the interlayer spacing and the entrance of the resin in the interlayer, the layer become thinner and the number of layers increases. When gas passes through the coating, it will encounter more lamellar structures. The gas diffusion in the transverse direction will increase, resulting in the increase of the length of transverse diffusion, and ultimately the path of gas penetrating the coating will greatly increase.

4. Conclusions

In this study, functional silicone resin coatings have excellent thermal properties and high crosslinking, which laid the foundation for improving the gas barrier of PET films. The lamellar sericite was intercalated modified to obtain a structure of 1.053 nm, which enlarged the interlayer spacing and improved the compatibility with silicone resin. It was dispersed in the silicone resin system to form complex "loop" structure, which increased the gas transverse diffusion path and prolonged the diffusion time. From the test of WVTR and OTR of modified PET films, it could be seen that this "loop" structure improves the gas barrier properties of PET films, and reduced the WVTR and OTR of PET films to 12.40 g / (m^2 • 24 h) and 29.91 cm^3/ (m^2 • 24 h • 0.1 MPa), respectively. This modified PET film has wide application prospects in food packaging because of its excellent gas barrier properties.

Acknowledgements

This work was financially supported by the National Natural Science Foundation of China (Grant No. 51673054), Harbin City Science and Technology Innovation Talent Foundation (Grant No. 2017RAYXJ003), and Shanghai Space Science and Technology Innovation Foundation (Grant No. SAST2017-114).

References

1. M. Yoshida, T. Tanaka, S. Watanabe, M. Shinohara, J. W. Lee and T. Takagi, *Surf. Coat. Technol.,* 2013, **174**, 1033-1037.
2. M. R. Galdi and L. Incarnato, *Packag. Technol. Sci.*, 2011, **24**, 89-102.
3. R. Willige, J. Linssen, M. Meinders, H. Stege and A. Voragen, *Food Addit. Contam.*, 2012, **19**, 303-313.
4. A. Rezaei, P. Carreau and A. Ajji, *ACS Appl. Mater. Interfaces*, 2014, **6**, 6415-6424.
5. G. Garnier, B. Yrieix, Y. Brechet and L. Flandin, *J. Appl. Polym. Sci.*, 2010, **11**, 3110-3119.
6. H.W. Liu, T. H. Chen, C. H. Chang, S.K. Lu, Y.C. Lin and D.S. Liu, *Appl. Sci.*, 2017, **7**, 56.
7. J. Wang, H. Chen, X. Wang and Z.Q. Yuan, *Appl. Phys. A.*, 2016, **122**, 967-974.
8. K. Goh, J. K. Heising, Y. Yuan, H.E. Karahan and L. Wei, *ACS Appl. Mater. Interfaces*, 2016, **8**, 9994-10004.
9. S. Farris, L. Introzzi, J. M. Fuentes-Alventosa, N. Santo, R. Rocca and L. Piergiovanni, *J. Agric. Food Chem.*, 2012, **60**, 782-790.
10. S. H. Bang, N. M. Hwang, H. L. Kim, *Microelectron. Eng.*, 2016, **166**, 39-44.
11. B. Yang, C. M. Parada and R. F. Storey, *Macromolecules*, 2016, **49**, 6173-6185.
12. R. Liu, X. Zhang, J. Zhu, X.Y. Liu, Z. Wang and Yan, JL, *ACS Sustainable Chem. Eng.*, 2015, **3**, 1313-1320.
13. X. Zhong, X. Pei, Y. Miao, L. He, and Huang, Q, *J. Eur. Ceram. Soc.*, 2017, **37**, 3263-3270.
14. K. Oshita, M. Yanagi and Y. Okada, *Surf. Coat. Technol.*, 2017, **325**, 738-745.
15. A. Vitale, M. G. Hennessy, O. K. Matar and J. T. Cabral, *Macromolecules*, 2014, **48**, 198-205.
16. B. Jiang, T. Zhang, Y. D. Huang, *Compos. Sci. Technol.,* 2017, **140**, 39-45.
17. M. W. Möller, D. A. Kunz, T. Lunkenbein, S. Sommer, A. Nennemann and J. Breu, *Adv. Mater.,* 2012, **24**, 2142-2147.
18. A. Khosravi, J. A. King, H. L. Jamieson and M. L. Lind, *Langmuir,* 2014, **30**, 13994-4003.
19. H. Liu, P. Bandyopadhyay, N. H. Kim, B. Moon, J. H. Lee, *Polym. Test.*, 2016, **50**, 49-56.
20. J. L. Achtyl, R. R. Unocic, L. Xu, Y. Cai, M. Raju and W. W. Zhang, *Nat. Commun.*, 2015, **6**, 6539.
21. H. Sehaqui, J. Kochumalayil, A. Liu, T. Zimmermann and L. A. Berglund, *ACS Appl. Mater. Interfaces*, 2013, **5**, 7613-7620.
22. Y. Tokudome, T. Hara, R. Abe and M. Takahashi, *ACS Appl. Mater. Interfaces,* 2014, **6**, 19355-19359.
23. H. Liu, T. Kuila, N. H. Kim, B. C. Ku and J. H. Lee, *J. Mater. Chem. A*, 2013, **1**, 3739-3746.
24. Y. H. Yang, L. Bolling, M. A. Priolo and J. C. Grunlan, *Adv. Mater.*, 2013, **25**, 503-508.
25. B. M. Yoo, H. J. Shin, H. W. Yoon and H. B. Park, *J. Appl. Polym. Sci.*, 2014, **131**, 39628.
26. S. Khalili, M. Masoomi, R. Bagheri, *J. Plast. Film Sheeting*, 2013, **29**, 39-55.
27. U. I. Uysal, D. Boyacı, S. Trabattoni, S. Tavazzi and S. Farris, *Nanomaterials*, 2017, **7**, 281.
28. N. Tenn, N. Follain, J. Soulestin, R. Cretois, S. Bourbigot and S. Marais, *J. Phys. Chem. C*, 2013, **117**, 12117-12135.
29. K. Oshita, S. Komiyama and S. Sasaki, *Tribol. Int.*, 2018, **123**, 349-358.
30. M. A. Priolo, D. Gamboa, K. M. Holder and J. C. Grunlan, *Nano Lett.*, 2010, **10**, 4970-4974.
31. B. Jiang, K. Y. Zhang, Q. F. Cai, T. Y. Zeng and M. F. Zhu, *Soft Mater.*, 2016, **14**, 288-296.
32. B. Jiang, T. Zhang, L.W. Zhao, Z. M. Xu, and Y. D. Huang, *J. Polym. Sci., Part A: Polym. Chem.*, 2017, **55**, 1696-1705.
33. P. Tzeng, C. R. Maupin and J. C. Grunlan, *J. Membr. Sci.*, 2014, **452**, 46-53.
34. H. Liu, P. Bandyopadhyay, N. H. Kim, B. Moon and J. H. Lee, *Polym. Test.*, 2016, **50**, 49-56.
35. H. Liu, T. Kuila, N. H. Kim, B. C. Ku and J. H. Lee, *J. Mater. Chem. A*, 2013, **1**, 3739-3746.